

ULTRA-SENSITIVE CARBON NANOTUBES FOR SINGLE-MOLECULE DETECTION OF DNA HYBRIDIZATION KINETICS USING CONDUCTANCE-BASED CORRELATION SPECTROSCOPY

S. Sorgenfrei¹, C.-Y. Chiu², C. Nuckolls², and K. Shepard¹

¹Department of Electrical Engineering, Columbia University, New York, New York, USA

²Department of Chemistry, Columbia University, New York, New York, USA

ABSTRACT

We present a label-free single-molecule based sensing platform using a carbon nanotube field-effect transistor. By point functionalizing a carbon nanotube through an electrochemical oxidation reaction, the conductance becomes sensitive and chemically reactive at a single point to which we can covalently attach a probe DNA molecule. Two-level fluctuations appear in the conductance of the carbon nanotube when it is immersed in a liquid buffer solution containing complementary target DNA. We show that the autocorrelation of the conductance can be used to extract DNA hybridization kinetics. The results are comparable to the one extracted through a hidden Markov model.

KEYWORDS

Carbon nanotube, single-molecule detection, autocorrelation, DNA hybridization kinetics

INTRODUCTION

Technological advances for probing single molecules have enabled the study of conformational changes and intramolecular dynamics. Fluorescence-based techniques are usually employed involving a fluorescence resonance energy transfer (FRET) pair. In particular, fluorescent correlation spectroscopy (FCS) has been extensively used for probing DNA hybridization dynamics at sub-millisecond resolution, especially in the hairpin loop configuration. These techniques, however, requires labeling with both donor and acceptor fluorophores [1].

In this work, we present the first label-free field-effect based sensing platform for probing biomolecular dynamics and employ it to monitor DNA hybridization. After probe DNA is covalently attached to a point defect in a carbon nanotube (CNT), we are able to measure two-level fluctuations in the nanotube conductance due to hybridization and melting of a complementary DNA target.

POINT FUNCTIONALIZED NANOTUBE

Carbon nanotubes around 1.4 nm are grown by chemical vapor deposition on a silicon wafer with a 300 nm thermal oxide. Titanium electrodes are patterned by standard photolithography for source and drain electrodes. Another lithography step is used to cover a selected nanotube and remove all others by an oxygen plasma etch, resulting in a single isolated nanotube with multiple electrodes. A platinum electrode is evaporated on the chip and the substrate is assembled in a

microfluidic setup with a polydimethylsiloxane (PDMS) mold as shown in Fig. 1. The advantage of having a microfluidic channel over the device is that different solutions can be easily exchanged and the device can be flushed. The setup is assembled in a standard 44-pin chip carrier so that multiple devices can be measured simultaneously.

The point defect in the nanotube is introduced by an electrochemical method, which consists of a conductance-controlled electrochemical-etching step in 1 M sulfuric acid (the potential is controlled by the on-chip platinum electrode) and then exposed to 6.5 mM potassium permanganate [2]. A typical conductance-based oxidation is shown in Fig. 2. Initially the conductance slowly decreases as the platinum voltage is decreased to below the threshold voltage of around -1 V. After a sudden jump down, the platinum voltage is increased to an intermediate voltage of -0.4 V. The voltage is kept at this potential during the exposure to potassium permanganate to avoid further oxidation or reduction, which could partially restore the conductance to the initial value. The potassium permanganate exposure turns the defect into a carboxylic acid functional group so that the probe DNA can be attached.

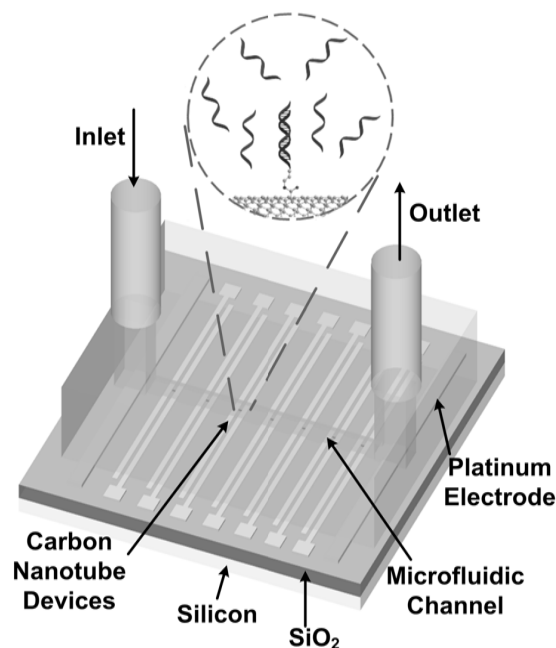


Figure 1: System Setup.

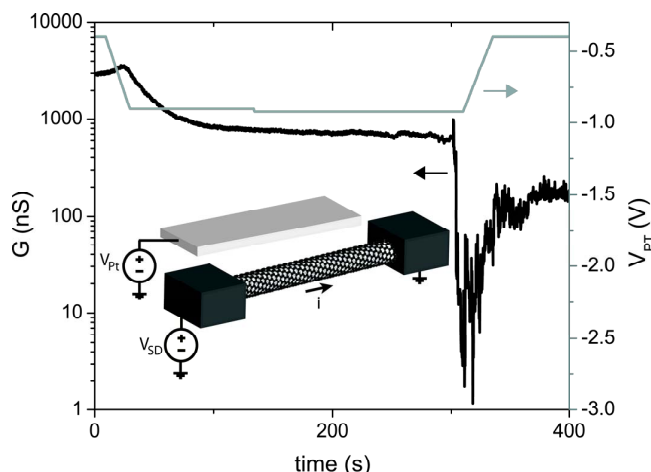


Figure 2: Conductance-controlled point defect creation.

We have further analyzed the defect of the nanotube by using scanning gate microscopy (SGM) [3]. In this method, the tip of an atomic force microscope is biased and the conductance of the nanotube is monitored at each position of the tip above the surface of the chip and the sensitivity of the device can be analysed. We have used a negatively biased tip (at -5V) 20 nm above the surface and the resulting SGM image is overlaid with the topography of the pristine semiconductor nanotube device in Fig. 3a, which clearly shows the Schottky barriers (darker areas). After point functionalization, the sensitivity becomes highly localized to a small region (Fig. 3b). In order to show that this defect is also chemically reactive, we have covalently attached a gold-labeled streptavidin. A gold particle can be found at the position of highest sensitivity in Fig. 3c.

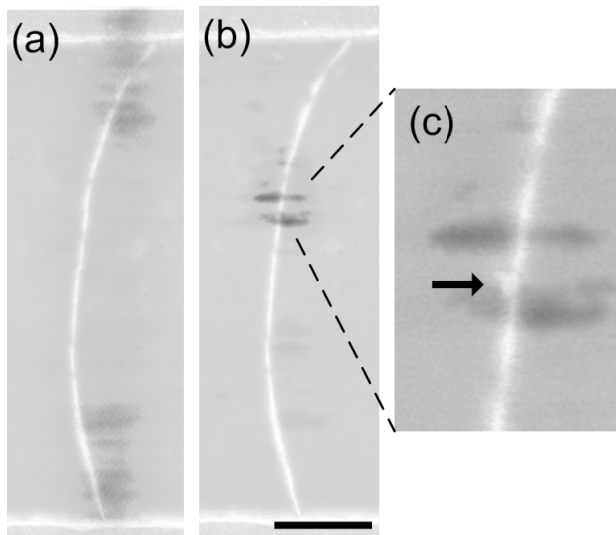


Figure 3: Combined SEM/SGM image before (a), after oxidation (b) and after coupling (c). Scale bar is 500nm.

DNA HYBRIDIZATION DYNAMICS

A 10-mer DNA probe molecule (NH₂-5'-GGAAAAAGG-3') is covalently attached to the freshly created carboxylic acid defect by a standard

coupling reaction using 1-ethyl-3-(3-dimethylamino propyl) carbodiimide (EDC) and sulpho-N-hydroxy-succinimide (sulpho-NHS). After thoroughly rinsing the device with deionized water, all subsequent measurements are taken in 1X PBS buffer (phosphate buffered saline) using the platinum electrode as a liquid gate and applying a small 100 mV source to drain bias. Without adding complementary target DNA, no particular features are observed and the device is dominated by flicker noise as shown in Fig. 4. After the addition of complementary target (1 μ M 5'-CCTTTTTC-3'), two-level fluctuations appear with a signal to noise ratio (SNR) of greater than 3 (shown in the lower real time trace in Fig. 4).

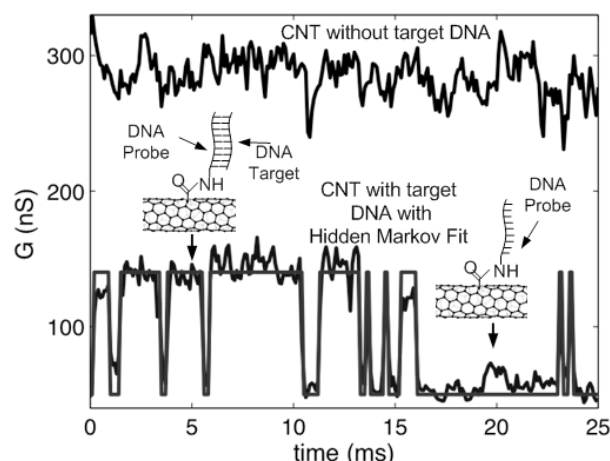


Figure 4: Real time measurement of CNT conductance.

We have previously analyzed the kinetics and thermodynamics of these fluctuations [4] and have interpreted the low conductance state as a device with duplex DNA (hybridized state) and the high conductance state as a device with solely probe DNA. This model is consistent with low temperature studies [5] and gas sensing experiments [6] using carbon nanotubes with defects where the defect represents a tunnel barrier or Frenkel-Poole emission. The attachment of a negatively charged DNA target molecule results in a barrier modulation, which yields the two-level fluctuations in the CNT conductance. In addition, there is a small overall decrease in the conductance, which we attribute to non-specific adsorption to the nanotube sidewall and the platinum electrode.

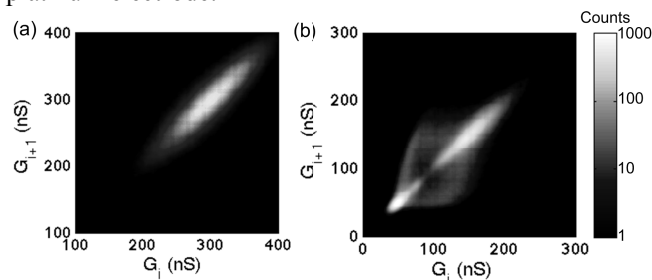


Figure 5: Time Lag Conductance plot before (a) and after (b) exposure to complementary DNA.

In order to clearly show the two states, we have used a time lag plot (TLP) [7], which is a two dimensional histogram of the conductance at consecutive data points. Fig. 5A shows the single state in the TLP with probe DNA only. Fig. 5B shows the two states after adding complementary DNA target.

EXTRACTION OF DNA KINETICS

One method to extract the kinetics is by idealizing the fluctuations using a hidden Markov model (HMM) and then exponentially fitting the dwell time histograms (Fig. 6a) [4]. There is a dominant kinetic mode characterized by very fast transitions (labeled “dominant kinetics” in Fig. 6a) and very slow transitions (labeled “non-ergodic intervals” in Fig. 6a). These long tails in the dwell time histograms are from time intervals where the fluctuations stop (as shown in the inset).

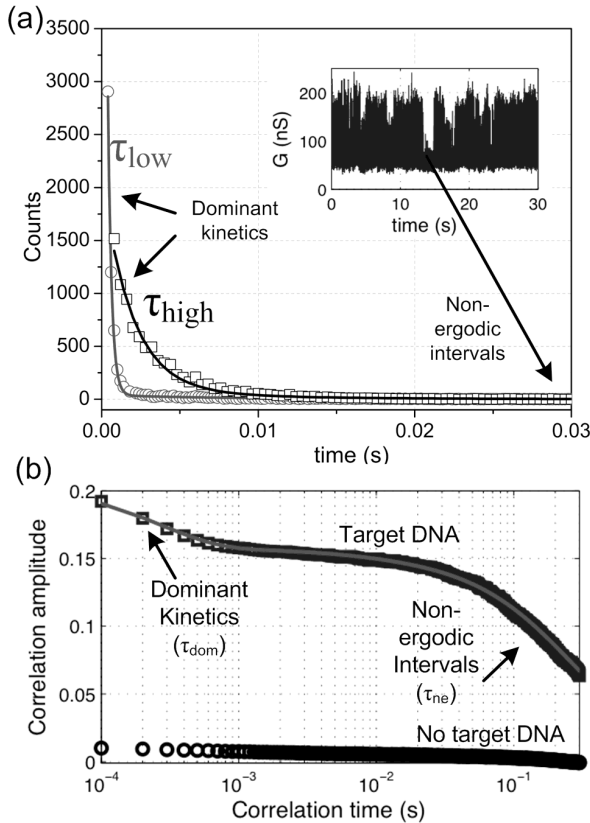


Figure 6: Kinetics extraction: HMM based (a) and autocorrelation based (b).

Another method to extract the kinetics is by taking the autocorrelation of the conductance. This method has been used for FCS based experiments when the FRET intensity levels cannot be clearly identified and the SNR ratio is low. The autocorrelation of the conductance $G(t)$ is given by

$$A(\tau) = \frac{\langle G(t)G(t+\tau) \rangle}{\langle G(t) \rangle^2} - 1 \quad (1)$$

We have plotted the autocorrelation of the

conductance in Fig. 6b for a device with no target DNA and then immersed in 1 μM target DNA. Ideally, the autocorrelation should fit to an exponential, but because of noise (mostly flicker noise in the carbon nanotube), a stretched exponential function was shown to best fit the data. Similar to FCS experiments, the autocorrelation can then be fit to

$$A(\tau) = A(0)e^{-\frac{t}{\tau}^\beta} \quad (2)$$

This equation has been used for fitting both the dominant and the non-ergodic time intervals as shown in Fig. 6b. The extracted dwell time τ is a combination of the high and low rates, given by $1/\tau = 1/\tau_{\text{high}} + 1/\tau_{\text{low}}$. Previously, we have shown that the melting curve of the DNA can be extracted by fitting a Gaussian function to the high and low conductance levels. The melting curve gives the ratio of the two rates as $M = \tau_{\text{high}}/(\tau_{\text{high}} + \tau_{\text{low}})$, which can be used to compute $k_{\text{hybridizing}} = (1-M)/\tau_{\text{dom}}$ and $k_{\text{melting}} = M/\tau_{\text{dom}}$.

In order to extract the melting curve, we have used a circular heater/refrigerator to control the temperature of a water reservoir, which in turn heats or cools down the temperature inside the microfluidic setup in Fig. 1 up to ± 0.1 $^{\circ}\text{C}$. The conductance of the CNT device was monitored using a current preamplifier for 8-minute time intervals at different temperatures. Fig. 7 shows the extracted melting curve from the Gaussian fits (inset of Fig. 7). We have only used time intervals without substantial non-ergodic sections in order to accurately extract the melting and hybridization rates.

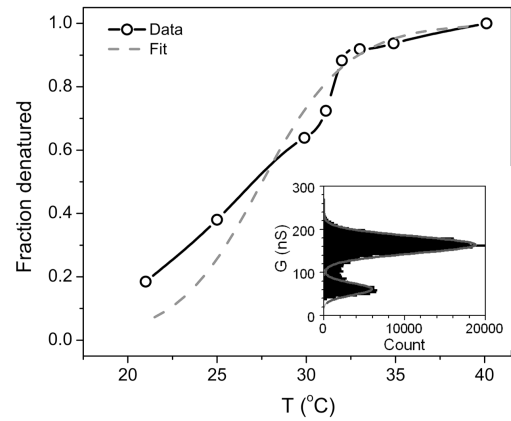


Figure 7: Melting curve. Inset shows example of Gaussian fits.

Finally, the kinetic rates at different temperatures can be extracted to create an Arrhenius plot to show the kinetic rates as an inverse function of temperature. Fig. 8a shows the Arrhenius plot using the Hidden Markov Model and Fig. 8b using autocorrelation. The Arrhenius plots using the two different methods are similar. Both plots show a shallow slope for both melting and hybridization rates at lower temperatures and then a sharp transition around the

melting temperature. The slight difference in the Arrhenius plots (the hybridization and melting rates show a greater difference both at high and low temperatures for the autocorrelation extracted one) is likely due to some residual non-ergodic intervals in the melting curve.

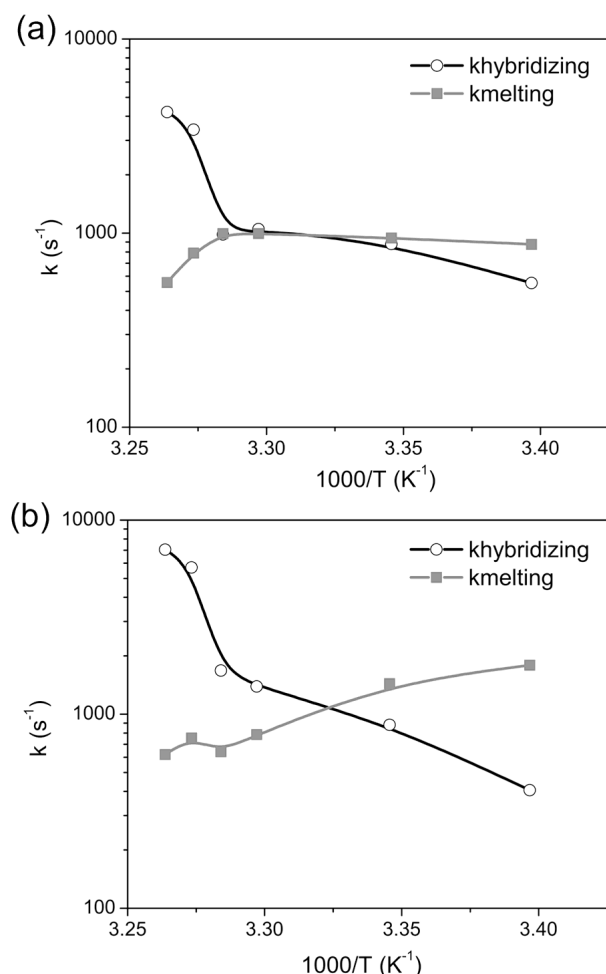


Figure 8: Arrhenius plots showing kinetic rates: kinetics were extracted based on (a) HMM and (b) autocorrelation.

CONCLUSION

We have presented a method to create a carboxylic acid defect in a carbon nanotube, which can be used to covalently attach biomolecules. As a proof of principle, we have studied the hybridization kinetics of a 10-mer DNA duplex. We have shown that both a hidden markov model and the autocorrelation of the conductance can be used to extract the kinetic rates and create an Arrhenius plot.

ACKNOWLEDGEMENTS

This work was supported in part by the National Science Foundation (grants ENG-0707748 and CHE-0641523). Additional support was provided by the New York State Office of Science, Technology, and Academic Research (NYSTAR). This work was also supported in part by the Office of Naval Research (grants N00014-09-01-0250 and N00014-09-1-1117) and by the

National Institutes of Health (grant R33-HG003089).

REFERENCES

- [1] M. Wallace, et al., "FRET Fluctuation Spectroscopy: Exploring the Conformational Dynamics of a DNA Hairpin Loop", *J. Phys. Chem. B*, Vol. 104, pp. 11551-11555, 2000
- [2] B. Goldsmith, et al., "Conductance-Controlled Point Functionalization of Single-Walled Carbon Nanotubes", *Science*, Vol. 315, pp. 77-81, 2007
- [3] A. Bachtold, et al., "Scanned probe microscopy of electronic transport in carbon nanotubes", *Phys. Rev. Lett.*, Vol. 84, pp. 6082-6085, 2000
- [4] S. Sorgenfrei, et al., "Label-free single-molecule detection of DNA hybridization kinetics using a carbon nanotube field-effect transistor", *Nature Nanotechnology*, Vol. 6, pp. 126-132, 2011
- [5] J. Mannik, et al., "Chemically Induced Conductance Switching in Carbon Nanotube Circuits", *Phys. Rev. Lett.*, Vol. 97, pp. 016601-1-016601-4, 2006
- [6] V. R. Khalap, et al., "Hydrogen Sensing and Sensitivity of Palladium-Decorated Single-Walled Carbon Nanotubes with Defects", *Nano Letters*, Vol. 10, pp. 896-901, 2010
- [7] T. Nagumo, et al., *Digest Tech. Papers, International Electron Devices Meeting (IEDM), December 7-9, 2009*, pp. 1-4

CONTACT

* S. Sorgenfrei; sorgenfrei@ee.columbia.com